



Species interactions may help explain the erratic periodicity of whooping cough dynamics

Samit Bhattacharyya^{a,b,*}, Matthew J. Ferrari^b, Ottar N. Bjørnstad^{b,c}

^a Mathematics, School of Natural Sciences, Shiv Nadar University, India

^b Center for Infectious Disease Dynamics, Pennsylvania State University, USA

^c Fogarty International Center, National Institutes of Health, Bethesda, MD, USA

ARTICLE INFO

Keywords:

Ecological interference
Age-structured model
Coexisting attractors
Bordetella

ABSTRACT

Incidence of whooping cough exhibits variable dynamics across time and space. The periodicity of this disease varies from annual to five years in different geographic regions in both developing and developed countries. Many hypotheses have been put forward to explain this variability such as nonlinearity and seasonality, stochasticity, variable recruitment of susceptible individuals via birth, immunization, and immune boosting. We propose an alternative hypothesis to describe the variability in periodicity – the intricate dynamical variability of whooping cough may arise from interactions between its dominant etiological agents of *Bordetella pertussis* and *Bordetella parapertussis*. We develop a two-species age-structured model, where two pathogens are allowed to interact by age-dependent convalescence of individuals with severe illness from infections. With moderate strength of interactions, the model exhibits multi-annual coexisting attractors that depend on the \mathcal{R}_0 of the two pathogens. We also examine how perturbation from case importation and noise in transmission may push the system from one dynamical regime to another. The coexistence of multi-annual cycles and the behavior of switching between attractors suggest that variable dynamics of whooping cough could be an emergent property of its multi-agent etiology.

1. Introduction

Historical records of childhood diseases exhibit complex patterns in dynamics. Dating back to the early twentieth century, case notifications of childhood diseases show a variety of temporal patterns, including regular cycles of variable period and apparently aperiodic dynamics (Anderson and May, 1991; Earn et al., 1998, 2000; London and Yorke, 1973; Rohani et al., 1999; Bhattacharyya et al., 2015). Moreover, the temporal epidemic pattern in a given location sometimes switches from one dynamical regime to another over long time-scales (Earn et al., 2000; Bolker and Grenfell, 1993; Rohani et al., 2002; Bauch and Earn, 2003). Historical surveillance often relies on clinical diagnosis, i.e., symptoms such as fever and rash, diarrhea, or ILI (influenza-like illness). Thus the dynamics observed may be due to the dynamics of the focal pathogen or interactions among the multiple pathogens that result in clinical syndrome. Complex temporal dynamics have been frequently documented in time series of whooping cough, which is a disease that can be caused by several strains of bacteria in the genus *Bordetella*. The two dominant species are *pertussis* and *parapertussis*. Changes in temporal patterns of whooping cough incidence are frequently seen even

within single populations governed by otherwise stable demographics (Broutin et al., 2005a). The dominant periodicity of whooping cough is annual or ranges from 3–5 years as documented in many settings: Portugal (Gomes et al., 1999), the United States (Hethcote, 1998; Tanaka et al., 2003), the United Kingdom (England and Wales) (Rohani et al., 1999; Anderson et al., 1984), and rural Senegal (Broutin et al., 2005b). A long time series of whooping cough reports from Copenhagen in the early 20th century provides an excellent illustration of variable periodicity; the time series of case notifications switches back and forth between long periods of annual cycles and periods of 3-year cycles, displaying distinct shifts between low-amplitude, noisy oscillations to high-amplitude well-defined cycles (Fig. 1).

Many hypotheses have been put forward to explain this erratic periodicity of whooping cough dynamics including noise in transmission (Rohani et al., 1999, 2002), slow changes in susceptible recruitment by birth and immunization (Earn et al., 2000; Broutin et al., 2010), and stochasticity in other epidemiological parameters such as latent and infectious periods (Nguyen and Rohani, 2008). Keeling et al. showed how seasonal forcing due to the binary nature of contact patterns during school closures introduces perturbations and switching

* Corresponding author at: Mathematics, School of Natural Sciences, Shiv Nadar University, India.

E-mail addresses: samit.b@snu.edu.in (S. Bhattacharyya), mjf283@psu.edu (M.J. Ferrari), onb1@psu.edu (O.N. Bjørnstad).

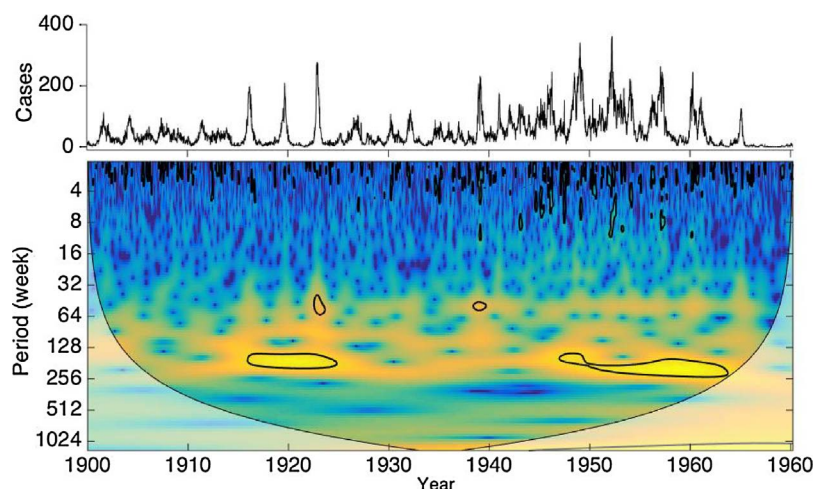


Fig. 1. Time series of the weekly reported cases in Copenhagen (upper panel), and wavelet decomposition of the square-root transformed reports (lower panel). Yellow areas of the wavelet plot indicate stronger support for cycles of the period identified on the left axis. The 5% significance level against red noise (indicated by yellow lighter shed) is shown as a thick contour. The other black line denotes the cone of influence (COI), where edge effects might distort the picture is shown as a lighter shade. Here, the dataset shows several lighter regions around the band of 1–3 year period, indicating stronger support for cycles of these respective periods. (For interpretation of the references to color in this figure legend, the reader is referred to the web version of this article.)

between different attractors (Keeling et al., 2001). Bauch and Earn performed perturbation analysis to show that non-resonant peaks in childhood disease, like measles, can arise due to transient dynamics in response to vaccination and slow changes in birth rate (Bauch and Earn, 2003). Recently, Lavine et al. proposed that models combining imperfect immunity with sensitive immune boosting can capture the change in age-incidence following vaccination and predict, under some circumstances, coexistence of cyclic and annual attractors (Lavine et al., 2013, 2011). Here, we explore a different mechanism based on an endogenous factor – species interactions via short-term isolation of host individuals – which gives an alternative explanation for the erratic dynamics of whooping cough.

Ecological interference through quarantine or convalescence has been shown to give rise to multi-annual outbreaks of diseases with distinct phase differences (Rohani et al., 1998, 2003). Here, we study the consequence of any such effects on the dynamics of two dominant etiological agents of whooping cough: *pertussis* and *parapertussis*. Though both bacteria can result in whooping cough, *parapertussis* generally results in less severe disease than *pertussis*. In the pre-vaccination era, *Bordetella parapertussis* accounted for between 0.1% and 10% of reported whooping cough cases (Lautrop, 1971; Miller et al., 1941). In Copenhagen between 1945 and 1970, *parapertussis* accounted for only (~0.049%, Fig. 2) of whooping cough cases (Lautrop, 1971). In this rare study that separated whooping cough incidence by etiological agents *pertussis* and *parapertussis* exhibit cycles of distinct 4-year periodicity, with a 2-year phase lag, suggesting a potential dynamical interaction despite the low absolute incidence of *parapertussis*. *Parapertussis* is starting to receive more attention because of better

diagnostic tools (like PCR (polymerase chain reaction)), improved surveillance methods, and increased awareness (He and Mertsola, 2008; Pittet et al., 2014; Rodgers et al., 2013). Recent observational studies have documented laboratory confirmed cases and outbreaks of *parapertussis* in a vaccinated population in Finland in 1985 (Mertsola, 1985) and from 1994–1997 (He et al., 1998), several states of United States from 2008–2011 (Cherry, 2005), China in 2011 (Zhang et al., 2014), and Canada in 2011 (Fisman et al., 2011).

Whooping cough disease can be caused by either species of bacterium; the time series that have been classically studied reflect infections with either and may reflect the dynamics of interactions between them. Infections by either of these two species can lead to severe disease, though the rate of severe illness due to *parapertussis* is much lower (Lautrop, 1971). Moreover, the severity of illness varies over age; children develop more severe disease than adults (British Society for the study of infection, 1997; Miller and Fletcher, 1976). Individuals with severe illness may self-quarantine at home or in hospital, thus limiting their interactions and potential for transmission. Thus, *interference* between these two pathogens may result when those with severe disease have lower exposure to the other species (e.g. during a period of convalescence) even though they may still be technically susceptible. Here, we develop a two-pathogen model where the strength of interaction between species arises from the age specific proportion of individuals with severe disease that will be temporarily removed due to a period of convalescence. We show that complex time series dynamics and multiple coexisting attractors in aggregate time series can arise from ecological interactions between pathogens. Further we show that random perturbations can cause jumps between those attractors. Thus our

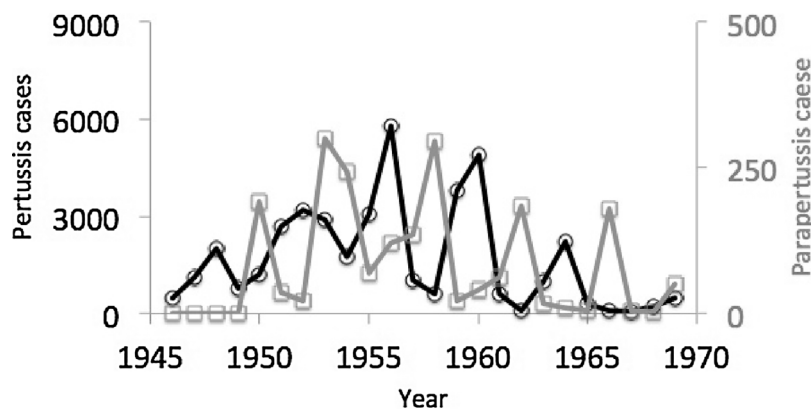


Fig. 2. Annual reported cases of *B. pertussis* and *B. parapertussis* in the city of Copenhagen and surrounding suburban counties from 1945 to 1969 (Lautrop, 1971). Both strains exhibit out-of-phase dynamics with 4 year periodicity, though *B. parapertussis* has much lower frequency than *B. pertussis*.

simple model is capable of generating qualitative pattern seen in whooping cough dynamics such as out of phase cycling of pertussis and parapertussis and switching between attractors.

2. Methods

2.1. Biological motivation and model structure

We develop a simple model of two interacting pathogens according to the classic SIRS model framework with age- and seasonally-dependent contact rates (Anderson and May, 1991). The two species, *Bordetella pertussis* and *B. parapertussis* in the model system are assumed to interact via quarantine or convalescence, where the individuals that develop severe disease are admitted to hospital or quarantined at home. This *short-term isolation* has been discussed in earlier literature and shown to have potential for causing ecological interference among pathogens (Rohani et al., 1998, 2003). There have been several studies of disease severity and hospital admission in whooping cough (British Society for the study of infection, 1997; Miller and Fletcher, 1976; Robinson et al., 1981; Heininger et al., 1994). Miller and Fletcher found, in a whooping cough outbreak (October 1974 to March 1975) in London, that more than 10% of cases developed severe disease and treated at hospital or home. They further found that the proportion considered severely ill was negatively correlated with age. In our model, we assume that the probability of severe disease decreases exponentially with age. Individuals with severe disease are assumed to be in a convalescent class that does not contribute to transmission. We also assume the average duration of illness to be the same for all age classes and relatively longer for *B. pertussis* than *B. parapertussis* (Miller and Fletcher, 1976). A detailed description of our model equations is given in Appendix A. Briefly, the individuals in the susceptible compartment, S , are susceptible to both of the infections I_i , $i = 1, 2$. Upon infection, individuals may or may not enter into the convalescence class C_i depending whether they develop severe illness. Both convalescent and non-convalescent illness are followed by a recovered class, during which individuals are immune.

In the simulation, we split the host population in 12 age groups: ≤ 1 , $1 - 2$, ..., $9 - 10$, $11 - 17$, and ≥ 17 years, and estimate the age-dependent transmission matrix using the contact-surface approach of Farrington and Whitaker (Farrington and Whitaker, 2005) for the age-specific force-of-infection (FOI) for pertussis. A brief description of the contact matrix estimation is given in the supplementary material. We assume that contact rates are sinusoidally forced and age-dependent (Schenzle, 1984). For both infections, immunity is temporary and individuals return to the susceptible class after immunity wanes. Other epidemiological parameters – infectious period, convalescence period, waning of immunity – are assumed to be age-independent (Table 1). The model equations are given in Appendix A.

We explore these dynamics across different transmission settings for both of the pathogens assuming the basic reproduction ratio \mathcal{R}_0 ranging from 9 to 15. \mathcal{R}_0 calculation for the age-specific model is described in the supplementary materials. We also compare the dynamics for three different types of convalescence: Scenario-I: a large fraction (γ_i^0) of infants experience severe disease, while the fraction decays rapidly with age (a_i^0); Scenario-II: a small fraction of infants experience severe disease with relatively slower decay rate; and scenario-III: constant proportion of severe disease across all age groups (Table 1). For scenario-I, we also checked the robustness of our results using a flat contact matrix among age groups.

2.2. Perturbation analysis

There are many possible sources of random noise or perturbations in infectious disease dynamics. We explore the effect of these perturbations through one mechanistic process, migration, and one phenomenological process, random fluctuation in transmission rate. We use

Table 1

Epidemiological parameters associated with two species pertussis and parapertussis (parameters are calibrated and referred from Miller and Fletcher (1976), Robinson et al. (1981), Huang and Rohani (2006), Hethcote (1999), Restif et al. (2008)).

| Parameter | Symbol | Value |
|---|--------------|----------|
| Total population | N | 100,000 |
| Birth rate | μ | 1/75 |
| Life expectancy | | 75 years |
| Infectious period of pertussis | $1/\eta_1$ | 14 days |
| Infectious period of parapertussis | $1/\eta_2$ | 10 days |
| Mean convalescent period of pertussis | $1/\delta_1$ | 30 days |
| Mean convalescent period of parapertussis | $1/\delta_2$ | 10 days |
| Duration of pertussis immunity | $1/\rho_1$ | 40 years |
| Duration of parapertussis immunity | $1/\rho_2$ | 35 years |

| | | Scenario-I | Scenario-II | Scenario-III |
|--|--------------|------------|-------------|--------------|
| Severity from pertussis at age class-I | γ_1^0 | 0.7 | 0.5 | 0.7 |
| Severity from parapertussis at age class-I | γ_2^0 | 0.1 | 0.1 | 0.1 |
| Exp. decay coefficient for pertussis | a_1^0 | 0.7 | 0.7 | 0 |
| Exp. decay coefficient for parapertussis | a_2^0 | 2 | 0.2 | 0 |

| | | Value (age class) |
|---|-----------------|-------------------|
| Force of infection (Kretzschmar et al., 2010) | $\lambda(t, a)$ | 0.13(1-4) |
| | | 0.12(5-9) |
| | | 0.15(10) |
| | | 0.2(11) |
| | | 0.14(12) |

these two different modes of perturbation to investigate the possibility of regime shifts of the system. We explore two different scenarios for case importations: imported cases within a specific age class, and imported cases distributed across a range of age classes. In the latter case, we consider the age distribution of importation to be either exponential, with higher probability in lower age groups, or normal with mean at the six-year age class and standard deviation 0.5. We consider the impact of both case importation scenarios under an assumption of age-structured mixing; we additionally consider the impact of the former case assuming uniform age-mixing (Supplement).

We finally consider the impact of noisy transmission on switching between attractors. We introduce a small pseudorandom noise (i.e., sampling the values from a uniform distribution over the interval $(0, 10^{-2})$) in the mean transmission rate of both infections for 5–6 years after the system has reached a stable attractor (Supplement). This is implemented as additive noise for a year on transmission. This noise is assumed to affect all ages in the same fashion.

3. Results

With baseline parameter values (Table 1) and fitted age-specific mixing (Supplement), age-specific convalescence introduces ecological interference between pertussis and parapertussis. While both pathogens exhibit irregular, small sized outbreaks at the lower \mathcal{R}_0 in the absence of an interaction, pertussis and parapertussis oscillate out-of-phase with a 4 year interepidemic period and 2 year phase difference when they interact with each other through age-dependent convalescence (Fig. 3), replicating the qualitative observations from pre-vaccination era pertussis-parapertussis dynamics in Copenhagen (Lautrop, 1971). We also run a comparison analysis both in the absence and presence of interaction under different strength of seasonality (Figure S3).

Interaction due to age-dependent convalescence results in a shift in the age distribution of cases of both pertussis and parapertussis compared to the no-interaction model (Fig. 4). In the no-interaction model the expected mean age of infection is (~ 4.5 yrs) for both pathogens; whereas the interaction model increases the mean age-of-infection of pertussis to 6.95 yrs and of parapertussis to 6 yrs. This pattern is

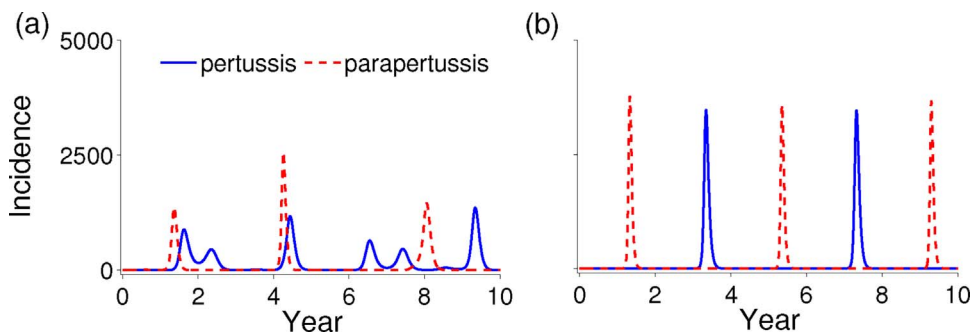


Fig. 3. Time series dynamics (aggregated both severe and non-severe cases) of two species in (a) absence and (b) presence of interactions via convalescence. The \mathcal{R}_0 of the two pathogens is 9 and amplitude of seasonality is 0.29. Other parameters values are given in Table 1. Although the incidence of pertussis and parapertussis is similar in (b), the actual reported cases for parapertussis is much less due to lower rates of severity from the disease compare to pertussis.

consistent with the observation of Lautrop (Lautrop, 1971) in Copenhagen of older mean age of infection for both pathogens and an older mean-age of infection in pertussis (7 years) compared to parapertussis (5 years). Description of the mean age of infection calculation is given in the supplementary material.

Most time series analyses of whooping cough do not differentiate between the two causative agents of the disease; thus we characterize the impact of interference on the aggregate time series dynamics of severe disease due to either pertussis or parapertussis. For the highest \mathcal{R}_0 (~15), if pertussis infection results in a high rate of severe disease in infants (scenario-I, Table 1), there are four different stable attractors in the aggregate time series that coexist with intertwined basins of attraction. In two attractors (blue and yellow), both species exhibit in-phase dynamics, while in the other two (cyan and red), they oscillate out-of-phase with relatively high fluctuations (Fig. 5). While three of the coexisting cycles are stable and biennial, attractor-III (yellow) lies on a complex manifold having two distinct branches (Figure S4). If the rate of severe disease due to pertussis infection is lower and decays more slowly with age (scenario II, Table 1), we also observe 3 different coexisting attractors: two biennial and one quasi-periodic (Figure S5).

To understand the main driver that causes these dynamics, we perform a simple scenario analysis at same \mathcal{R}_0 (~15) to isolate the impacts of age-structured disease severity and age-structured transmission. With constant disease severity across age (scenario III, Table 1), but age-specific transmission, the aggregate dynamics of whooping cough exhibit 4 different biennial, higher order, and quasi-periodic attractors (Figure S6). If we assume age-structured disease severity and a flat age-specific contact matrix the model generates two coexisting regimes: one biennial and one quasi-periodic (Figure S7). Lastly, a simple two-disease model with no age structure in disease severity and transmission produces a single type of attractor of irregular pattern for the entire basin of attraction (Figure S8). Thus, the scenario analysis indicates that age-specific disease severity can generate multiple coexisting cycles with highly intertwined basin of attractors.

At lower transmission rates, the model shows similar qualitative features. At $\mathcal{R}_0 \sim 10 - 14$, the model with age-structure in both severity and transmission, exhibits different 2, 4, 6 and 8 periodic, quasi-

periodic attractors and other complex attractors (Figure S9–S12). For example, at $\mathcal{R}_0 \sim 9$ with higher seasonality and rates of severe disease similar to scenario I (Table 1), the system exhibits stable coexisting attractors of relatively large inter-epidemic periods – 4-periodic, 8-periodic and a 8-year quasi-periodic in more dense intertwined basins (Figure S13). Our sensitivity analysis indicates that multi-annual attractors of two different types coexist for all possible values of \mathcal{R}_0 : (i) stable attractors where pertussis and parapertussis oscillate out of phase with phase-locking, and (ii) the two pathogens are exhibiting in-phase cycles lying on either stable or unstable manifolds. Hence multiple coexisting attractors of different periods are an emergent property of such interacting disease systems. Thus, ecological interaction between the two bacteria that cause whooping cough may produce the variable dynamics observed in the aggregate time series.

In instances where multiple stable attractors coexist with finely intertwined basins of attraction, perturbations can result in jumps between them (Bauch and Earn, 2003; Earn et al., 2000). Here, we consider perturbations due to case importation for a model with age-specific disease severity (scenario I) and age-specific mixing. Depending on the magnitude and the age group of case importation, the system jumps from the baseline attractor to other attractors (Fig. 6). We note that importation of older cases is less likely to result in a dynamic shift from the baseline attractor because older cases are less likely to result in severe disease and thus ecological interference. If the model assumes a flat contact matrix, the system exhibits a qualitatively similar pattern of attractor switching that changes with the magnitude and mean age of imports (Figure S14). Thus the dynamic effect of case importation depends on the age class of the imported individuals. In fact, it has two competing effects on the interaction dynamics; introducing more pertussis cases not only increases the transmission of pertussis but also decreases the relative force of infection of parapertussis. Thus case importation inhibits the impact of interaction via convalescence and pushes the dynamics to a different regime.

A more realistic setting would be that imports are drawn from some distribution of age classes. We considered scenarios where the migrant population is composed primarily of young children (exponential distribution), or primarily of older children (normal distribution with

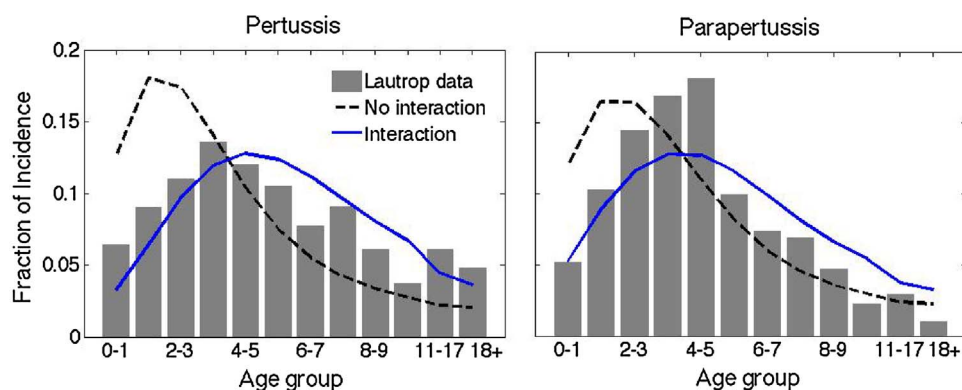


Fig. 4. Comparison of age distribution of incidences from Lautrop data (Lautrop, 1971), no-interaction model and interaction model. The interaction model exhibits the age-shift as shown in Lautrop data. A simple SIR model with specific features and parameter values of each species has been simulated as no-interaction model.

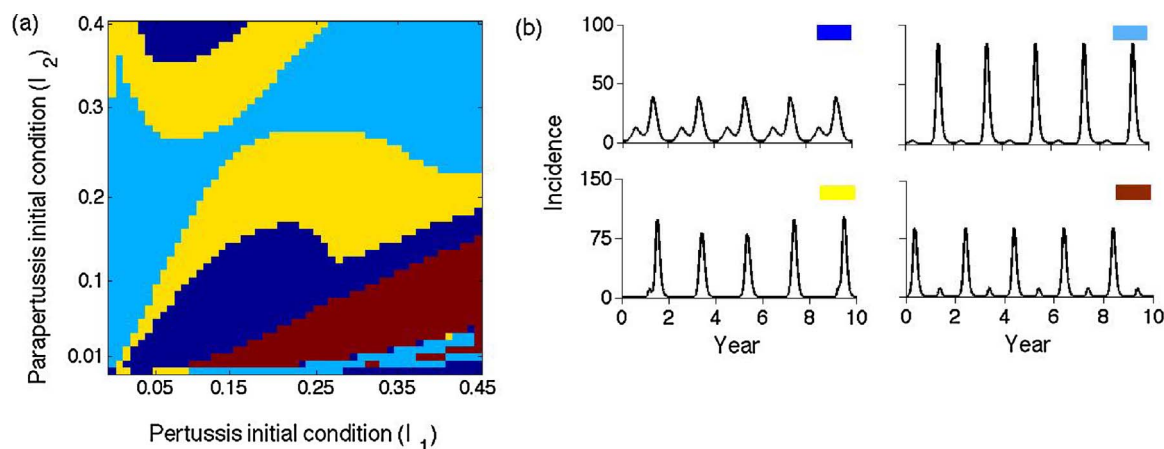


Fig. 5. Dynamics of the disease at higher R_0 : (a) basin of attraction and (b) four different coexisting attractors (attractor-I (blue), attractor-II (cyan), attractor-III (yellow), attractor-IV (red)). R_0 is 15.85 for both pathogens and amplitude of seasonality is 0.17. Time series shown in the figure are combined incidence of pertussis and paraptussis. For details, see the text. (For interpretation of the references to color in this figure legend, the reader is referred to the web version of this article.)

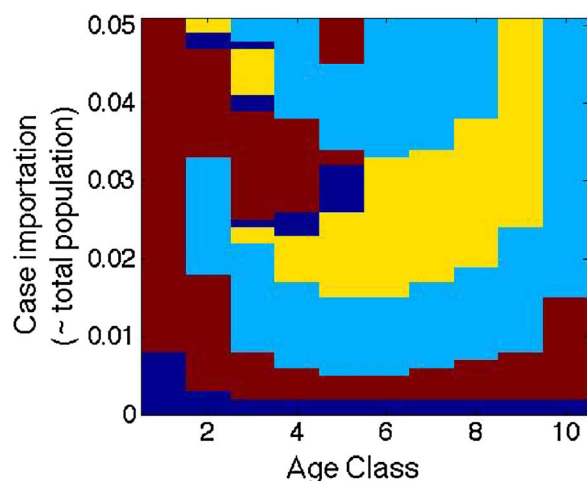


Fig. 6. Switching of attractors due to case importation, where the underlined contact matrix is structured. The color representation and parameter values are same as in Fig. 5. The baseline attractor for the entire simulation is attractor-I (blue), the attractor at zero importation. (For interpretation of the references to color in this figure legend, the reader is referred to the web version of this article.)

mean 6 years). Here we allowed the model to reach equilibrium in each of the 4 coexisting attractors (see Fig. 5) by simulating from different initial conditions, and then introduced migrants (0.004 proportion of population size) drawn from either of the two age distributions. Using these more realistic scenarios yields qualitatively similar results to those illustrated in Fig. 6 (see Supplement, Figure S15, S16).

Basin jumps are also observed when we perturb the system by introducing noise in transmission (Figure S17). Depending on the strength and duration of the noise, the damping rate and oscillation period of the transient solution may vary. We can obtain the damping rate and the oscillation period by computing poincaré sections and eigenvalue analysis near the stable attractor (Bauch and Earn, 2003). The attractor to which the system switches is sensitive to the strength, duration, and the time point where the noise is introduced. Nonetheless, this perturbation analysis indicates that simple interactions between species coupled with perturbation may contribute to the variable dynamics of whooping cough observed in space and time.

4. Discussion

Understanding the complex incidence patterns of childhood diseases is still an exciting issue to mathematical ecologists and epidemiologists.

Rarely are disease time series resolved to the level of species or strains in diseases of multiaetiological origin, including for example, whooping cough (caused by bacteria in the genus of *Bordetella*), croup (caused by various viral strains within paramyxoviridae), and ILI (Influenza-like illness, caused by a range of viruses including influenza and rhinovirus strains). Thus the aggregate time series of disease that is reported may represent dynamics arising from the interaction of multiple agents. Previous attempts at explaining long-term whooping cough epidemics have argued for several exogenous and endogenous factors such as demographic factors, noise in transmission and seasonality, stochasticity and immune boosting (Bauch and Earn, 2003; Hethcote, 1998, 1999; Lavine et al., 2013; Metcalf et al., 2009; Rohani et al., 2000), but assume single dominant etiological agent.

Here we studied the temporal dynamics of a two species model and showed how species interactions through ecological interference can result in complicated aggregate dynamics. We combine two processes, species interactions and perturbation analysis of attractors, to study the complex time series dynamics that may arise in multi-pathogen diseases. The age-dependent convalescence isolates infected individuals (with severe disease) from the chain of circulation and thus affects the transmission of the other pathogen in two different ways: it limits the host resources (i.e., susceptibles), and increases the relative FOI of the other pathogen. Thus two interacting feedback mechanisms balance each other to give rise to sustained oscillations in each pathogen. These interference signatures are consistent with general theory of ecological interference (Huang and Rohani, 2006). We find that a model of interaction via ecological interference can reproduce three key qualitative observations of whooping cough dynamics: out of phase cycles between pertussis and paraptussis, a higher mean age of infection in pertussis, and complex time series dynamics in the aggregate case reports of whooping cough.

Our results show that moderate interaction of two pathogens can give rise to coexistence of multi-annual attractors, and simple perturbations, like case-importation or noise in transmission, can lead to switches in the dynamics from one regime to another. Although, we have considered the underlying age-structure to match the qualitative pattern of the Lautrop data on pertussis and paraptussis (Lautrop, 1971), the presence of coexisting attractors is also observed with other age-structured population and contact matrix such as that from the POLYMOD studies (Mossong et al., 2008) (see Supplement Figure S18). We also experiment with different duration of immunity for both of pathogens. For example, we consider duration of immunity from pertussis and pertussis is 20 years and 15 years, respectively. Regardless of pattern, the system shows similar variable dynamics of annual and biennial attractors (Figure S19). Although, we have explored the

mechanisms with models under sinusoidal forcing, we believe that “term-time, age-specific” forcing might also have similar effect in producing variable dynamics. There are previous studies of attractor switching in a single-species model of whooping cough (Lavine et al., 2013), but our result provides an additional hypothesis for whooping cough irregularities.

A limitation of our model is that we do not explicitly consider the consequences of co-infection with both pathogens on case reports of whooping cough. Individuals with co-infections would likely also be convalescent, but their proportion is at such a low value in our model output, we did not implement the convalescence mechanism for co-infected population. Recent laboratory studies of these two pathogens in the mouse model indicate that *B. parapertussis* may have a competitive advantage over *B. pertussis* through cross-protective immunity (Zhang et al., 2009), though it still remains controversial, at least in human populations (Lautrop, 1971; Khelef et al., 1993). For example, studies by Lautrop pointed out that 73 children became infected with both *B. pertussis* and *B. parapertussis* over a 17-year period (1953–1970) in Denmark, and concluded that “preventive cross-immunity ...does not exist” (Lautrop, 1971). In this paper, we do not consider any cross-protective immunity between these two species. Restif et al. (2008) considered the asymmetric cross-immunity between *B. pertussis* and *B. parapertussis* and discuss conditions that allow the coexistence of the two etiological agents. An analogous situation is when immunization is considered in such a multi-pathogen framework. The acellular vaccine

protects from pertussis, but not parapertussis. This is an interesting future question that vaccination, which may have an asymmetric effect on the system, can impact the interactions of these two species. For example, offset of age-distribution and positive correlation of pertussis and parapertussis incidence in Massachusetts (1990–2008) are likely due to pertussis vaccine-induced immunity in the population (Lavine et al., 2010).

Many reported diseases can result from multiple etiological agents: e.g. diarrheal disease, influenza like illness, meningococcal meningitis. Analysis of the aggregate time series of case reports may cloak the interactions among these potentially competing agents (Bhattacharyya et al., 2015). Here we have shown that the complex time series phenomena observed in one multi-agent disease, whooping cough, could be a consequence of interactions between the two dominant bacterial agents. Thus, consideration of the influence of competing etiological agents, and improved diagnostics to allow species specific surveillance, may improve our understanding of the dynamics and predictability of multi-agent infections.

Acknowledgements

We would like to acknowledge the support from Bill and Melinda Gates Foundation. O.N.B. was additionally funded by Research and Policy for Infectious Disease Dynamics (RAPIDD) program of the Science & Technology Directorate.

Appendix A. Two disease age-structured Model

Let S, I_i, I_m, C_i denote respectively, the proportion of susceptible to both species, infected by species i , infected by both species and convalescence due to disease i respectively. S_i, J_i are the proportion of individuals susceptible to disease i , infected by disease i respectively, but immune to the other disease. R denotes the recovered class immune to both species. We assume immunity to be temporary, where individuals return to the respective susceptible class once immunity wanes. According to the simplified epidemiological life history described, the interaction by the two pathogens can be described by following set of partial differential equations:

$$\begin{aligned}
 \left\{ \frac{\partial}{\partial t} + \frac{\partial}{\partial a} \right\} S(t, a) &= -(\lambda_1(t, a) + \lambda_2(t, a) + \mu)S + \rho_2 S_1 + \rho_1 S_2, \\
 \left\{ \frac{\partial}{\partial t} + \frac{\partial}{\partial a} \right\} I_1(t, a) &= \lambda_1(t, a)S - \lambda_2(t, a)I_1 - (\gamma_1(a) + \eta_1 + \mu)I_1, \\
 \left\{ \frac{\partial}{\partial t} + \frac{\partial}{\partial a} \right\} I_2(t, a) &= \lambda_2(t, a)S - \lambda_1(t, a)I_2 - (\gamma_2(a) + \eta_2 + \mu)I_2, \\
 \left\{ \frac{\partial}{\partial t} + \frac{\partial}{\partial a} \right\} I_m(t, a) &= \lambda_2(t, a)I_1 + \lambda_1(t, a)I_2 - (\eta_1 + \eta_2 + \mu)I_m, \\
 \left\{ \frac{\partial}{\partial t} + \frac{\partial}{\partial a} \right\} C_1(t, a) &= \gamma_1(a)I_1 - (\delta_1 + \mu)C_1, \\
 \left\{ \frac{\partial}{\partial t} + \frac{\partial}{\partial a} \right\} C_2(t, a) &= \gamma_2(a)I_2 - (\delta_2 + \mu)C_2, \\
 \left\{ \frac{\partial}{\partial t} + \frac{\partial}{\partial a} \right\} S_1(t, a) &= \eta_2 I_2 + \delta_2 C_2 - (\lambda_1(t, a) + \mu)S_1 - \rho_2 S_1 + \rho_1 R \\
 \left\{ \frac{\partial}{\partial t} + \frac{\partial}{\partial a} \right\} S_2(t, a) &= \eta_1 I_1 + \delta_1 C_1 - (\lambda_2(t, a) + \mu)S_2 - \rho_1 S_2 + \rho_2 R \\
 \left\{ \frac{\partial}{\partial t} + \frac{\partial}{\partial a} \right\} J_1(t, a) &= \lambda_1(t, a)S_1 + \eta_2 I_m - (\eta_1 + \mu)J_1, \\
 \left\{ \frac{\partial}{\partial t} + \frac{\partial}{\partial a} \right\} J_2(t, a) &= \lambda_2(t, a)S_2 + \eta_1 I_m - (\eta_2 + \mu)J_2, \\
 \left\{ \frac{\partial}{\partial t} + \frac{\partial}{\partial a} \right\} R(t, a) &= \eta_1 J_1 + \eta_2 J_2 - (\rho_1 + \rho_2 + \mu)R,
 \end{aligned} \tag{1}$$

where the age-dependent convalescence rate for disease i is given by

$$\gamma_i(a) = \frac{\eta_i \gamma_i^0 \exp(a_i^0(1-a))}{1 - \eta_i \gamma_i^0 \exp(a_i^0(1-a))}, \quad i = 1, 2 \tag{2}$$

A schematic of the disease process between several epidemiological compartments are given in the supplementary (Figure S2). The force of infection of disease i at cohort a and time t is given by

$$\lambda_i(t, a) = \int_0^\infty \frac{\beta(a, \alpha)}{N(a)} (I_i(t, a) + J_i(t, a) + I_m(t, a)) d\alpha, \quad i = 1, 2 \tag{3}$$

and the boundary conditions $S(t, 0) = \mu N$, $N = \int_0^\infty N(a) da$ is the total population. The transmission is seasonally forced with sinusoidal forcing. Detailed parameter descriptions and values are given in Table 1. Estimation of transmission matrix $\beta(i, j)$ is discussed in supplementary.

Appendix B. Supplementary data

Supplementary data associated with this article can be found, in the online version, at <https://doi.org/10.1016/j.epidem.2017.12.005>.

References

- Anderson, R.M., May, R.M., 1991. *Infectious Diseases of Humans*. Oxford University Press.
- Anderson, R.M., Grenfell, B.T., May, R.M., 1984. Oscillatory fluctuations in the incidence of infectious disease and the impact of vaccination: time series analysis. *J. Hyg. (Lond.)* 93, 587–608.
- Bauch, C.T., Earn, D.J.D., 2003. Transients and attractors in epidemics. *Proc. R. Soc. B Lond.* 270, 1573–1578.
- Bhattacharyya, S., Gesteland, P.H., Korgenski, K., Bjørnstad, O.B., Adler, F.R., 2015. Cross-immunity between strains explains the dynamical pattern of paramyxoviruses. *PNAS* 112, 13396–13400.
- Bolker, B.M., Grenfell, B.T., 1993. Chaos and biological complexity in measles dynamics. *Proc. R. Soc. B Lond.* 251, 75–81.
- British Society for the study of infection, 1997. Whooping cough a retrospective study of hospital admissions. *J. R. Coll. Gen. Pract.* 27, 93–95.
- Broutin, H., Guegan, J.F., Elguero, E., Simondon, F., Cazelles, B., 2005a. Large-scale comparative analysis of pertussis population dynamics: periodicity, synchrony, and impact of vaccination. *Am. J. Epidemiol.* 161, 1159–1167.
- Broutin, H., Mantilla-Beniers, N., Simondon, F., et al., 2005b. Epidemiological impact of vaccination on the dynamics of two childhood diseases in rural Senegal. *Microbes Infect.* 7, 593–599.
- Broutin, H., Viboud, C., Grenfell, B.T., Miller, M.A., Rohani, P., 2010. Impact of vaccination and birth rate on the epidemiology of pertussis: a comparative study in 64 countries. *Proc. R. Soc. Lond. B* 277, 3239–3245.
- Cherry, J.D., 2005. The epidemiology of pertussis: a comparison of the epidemiology of the disease pertussis with the epidemiology of *Bordetella pertussis* infection. *Pediatrics* 115 (5), 1422–1427.
- Earn, D.J.D., Rohani, P., Grenfell, B.T., 1998. Persistence, chaos and synchrony in ecology and epidemiology. *Proc. R. Soc. Lond. B* 265, 7–10.
- Earn, D.J.D., Rohani, P., Bolker, B.M., Grenfell, B.T., 2000. A simple model for complex dynamical transitions in epidemics. *Science* 287, 667–670.
- Farrington, C.P., Whitaker, H.J., 2005. Contact surface models for infectious diseases. *J. Am. Stat. Assoc.* 100 (470), 370–379.
- Fisman, D.N., Tang, P., Hauck, T., et al., 2011. Pertussis resurgence in Toronto, Canada: a population-based study including test-incidence feedback modeling. *BMC Public Health* 11 (1), 694.
- Gomes, M.C., Gomes, J.J., Paulo, A.C., 1999. Diphtheria, pertussis, and measles in Portugal before and after mass vaccination: a time series analysis. *Eur. J. Epidemiol.* 15, 791–798.
- He, Q., Mertsola, J., 2008. Factors contributing to pertussis resurgence. *Future Microbiol.* 3 (3), 329–339.
- He, Q., Viljanen, M.K., Arvilommi, H., Aittanen, B., Mertsola, J., 1998. Whooping cough caused by *Bordetella pertussis* and *Bordetella parapertussis* in an immunized population. *JAMA* 280 (7), 635–637.
- Heininger, U., Stehr, K., Schmitt-Grohé, S., Lorenz, C., Rost, R., Christenson, P., Uberall, M., Cherry, J., 1994. Clinical characteristics of illness caused by *Bordetella parapertussis* compared with illness caused by *Bordetella pertussis*. *Pediatr. Infect. Dis. J.* 13 (4), 306–309.
- Hethcote, H.W., 1998. Oscillations in an endemic model for pertussis. *Can. Appl. Math. Q.* 6, 61–88.
- Hethcote, H., 1999. Simulations of pertussis epidemiology in the United States: effects of adult booster vaccinations. *Math. Biosci.* 158, 47–73.
- Huang, Y., Rohani, P., 2006. Age-structured effects and disease interference in childhood infections. *Proc. R. Soc. B* 273, 1229–1237.
- Keeling, M.J., Rohani, P., Grenfell, B.T., 2001. Seasonally forced disease dynamics explored as switching between attractors. *Physica D: Nonlinear Phenom.* 148 (3), 317–335.
- Khelef, N., Danve, B., Quentin-Millet, M.J., Guiso, N., 1993. *Bordetella pertussis* and *Bordetella parapertussis*: two immunologically distinct species. *Infect. Immun.* 61 (2), 486–490.
- Kretzschmar, M., Teunis, P.F.M., Pebody, R.G., 2010. Incidence and reproduction numbers of pertussis: estimates from serological and social contact data in five European countries. *PLoS Med.* 7 (6), e1000291. <http://dx.doi.org/10.1371/journal.pmed.1000291>.
- Lautrop, H., 1971. Epidemics of parapertussis, 20 years' observation in Denmark. *Lancet* (June), 1195–1198.
- Lavine, J., Broutin, H., Harvill, E.T., Bjørnstad, O.N., 2010. Imperfect vaccine-induced immunity and whooping cough transmission to infants. *Vaccine* 29 (1), 11–16.
- Lavine, J.S., King, A.A., Bjørnstad, O.N., 2011. Natural immune boosting in pertussis dynamics and the potential for long-term vaccine failure. *Proc. Natl. Acad. Sci.* 108 (17), 7259–7264.
- Lavine, J.S., King, A.A., Andreasen, V., Bjørnstad, O.N., 2013. Immune boosting explains regime-shifts in prevaccine-era pertussis dynamics. *PLOS ONE* 8 (8), e72086. <http://dx.doi.org/10.1371/journal.pone.0072086>.
- London, W., Yorke, J.A., 1973. Recurrent outbreaks of measles, chickenpox and mumps. I. Seasonal variation in contact rates. *Am. J. Epidemiol.* 98, 469–482.
- Mertsola, J., 1985. Mixed outbreak of *Bordetella pertussis* and *Bordetella parapertussis* infection in Finland. *Eur. J. Clin. Microbiol.* 4 (2), 123–128.
- Metcalfe, C.J.E., Bjørnstad, O.N., Grenfell, B.T., Andreasen, V., 2009. Seasonality and comparative dynamics of six childhood infections in pre-vaccination Copenhagen. *Proc. Biol. Sci.* 276, 4111–4118.
- Miller, C.L., Fletcher, W.B., 1976. Severity of notified whooping cough. *Br. Med. J.* 1, 117–119.
- Miller, J.J., Saito, T.M., Silverberg, R.J., 1941. Parapertussis: clinical and serological observations. *J. Pediatr.* 19, 229–240.
- Mossong, J., Hens, N., Jit, M., Beutels, P., Auranen, K., Mikolajczyk, R., Massari, M., Salmaso, S., Tomba, G.S., Wallinga, J., Heijne, J., 2008. Social contacts and mixing patterns relevant to the spread of infectious diseases. *PLoS Med.* 5 (3), e74.
- Nguyen, H.T.H., Rohani, P., 2008. Noise, nonlinearity and seasonality: the epidemics of whooping cough revisited. *J. R. Soc. Interface* 5, 403–413.
- Pittet, L.F., Emonet, S., François, P., et al., 2014. Diagnosis of whooping cough in Switzerland: differentiating *Bordetella pertussis* from *Bordetella holmesii* by polymerase chain reaction. *PLOS ONE* 9 (2), e88936.
- Restif, O., Wolfe, D.N., Goebel, E.M., Bjørnstad, O.N., Harvill, E.T., 2008. Of mice and men: asymmetric interactions between *Bordetella* pathogen species. *Parasitology* 135 (13), 1517–1529.
- Robinson, D.A., Mandal, B.K., Ironside, A.K., Dunbar, E.M., 1981. Whooping cough – a study of severity in hospital cases. *Arch. Dis. Child.* 56, 687–691.
- Rodgers, L., Martin, S.W., Cohn, et al., 2013. Epidemiologic and laboratory features of a large outbreak of pertussis-like illnesses associated with co-circulating *Bordetella holmesii* and *Bordetella pertussis* in Ohio, 2010–2011. *Clin. Infect. Dis.* 56 (3), 322–331.
- Rohani, P., Earn, D.J.D., Finkenstadt, B.F., Grenfell, B.T., 1998. Population dynamic interference among childhood diseases. *Proc. R. Soc. Lond. B* 265, 2033–2041.
- Rohani, P., Earn, D.J.D., Grenfell, B.T., 1999. Opposite patterns of synchrony in sympatric disease metapopulations. *Science* 286, 968–971.
- Rohani, P., Earn, D.J.D., Grenfell, B.T., 2000. The impact of immunisation on pertussis transmission in England & Wales. *Lancet* 355, 285–286.
- Rohani, P., Keeling, M.J., Grenfell, B.T., 2002. The interplay between determinism and stochasticity in childhood diseases. *Am. Nat.* 159, 469–481.
- Rohani, P., Green, C.J., Mantilla-Beniers, N.B., Grenfell, B.T., 2003. Ecological interference among fatal infections. *Nature* 422, 885–888.
- Schenzle, D., 1984. An age structured model of pre- and post-vaccination of measles transmission. *IMA J. Math. Appl. Med. Biol.* 1, 169–191.
- Tanaka, M., Vitek, C., Pascual, F., Bisgard, K., Tate, J., Murphy, T.V., 2003. Trends in pertussis among infants in the United States, 1980–1999. *JAMA* 290, 2968–2975.
- Zhang, X., Rodriguez, M.E., Harvill, E.T., 2009. O antigen allows *B. parapertussis* to evade *B. pertussis* vaccine-induced immunity by blocking binding and functions of cross-reactive antibodies. *PLoS ONE* 4 (9), e6989. <http://dx.doi.org/10.1371/journal.pone.0006989>.
- Zhang, Q., Zundong, Y., et al., 2014. Prevalence of asymptomatic *Bordetella pertussis* and *Bordetella parapertussis* infections among school children in China as determined by real time PCR: a cross-sectional study. *Scand. J. Infect. Dis.* 1–8. <http://dx.doi.org/10.3109/00365548.2013.878034>.